Solving the Orientation-Duality Problem for a Circular Feature in Motion

D. He and B. Benhabib

***Abstract*— Circular features have been commonly used in numerous computer vision application areas for three-dimensional (3-D) pose estimation. However, the estimation of such a feature's pose from two-dimensional (2-D) image coordinates results in an orientation-duality problem. Namely, although the 3-D position of the circle's center can be uniquely identified, the solution process yields two different feasible orientations, of which only one is the true solution. This duality problem is normally addressed through the acquisition of a second image in the case of a "static" feature. This solution, however, would not be applicable to "features in motion." In this paper, several methods are presented for the solution of the orientation-duality problem for circular features that are in motion. The first approach is applicable to those features moving on a 3-D line with constant orientation or to those which are moving on a plane with general motion. The second approach relies on the existence of additional object features, such as points or lines, which are coplanar to the circular feature. In this case, the circular feature can undergo an arbitrary 3-D motion. Experimental results verify the validity of the proposed methods.**

I. Introduction

Motion study from consecutive images is one of the key issues in the development of a vision system for moving-object recognition. There exist two common approaches: Feature-based methods and optical-flow methods. Feature-based techniques require that correspondence be established between a sparse set of features extracted from one image with those extracted from the next image in the sequence. Many features have been used to establish such correspondence, including points, lines, planes, conics and combination of these features [1]–[6]. Although numerous techniques have been established for extracting and establishing feature correspondence, they are normally suitable for simple situations (i.e., nongeneral motions) [7].

Amongst available features, use of an image sequence of a single point or of a line segment may not be sufficient for estimating all the necessary three-dimensional (3-D) motion parameters. Therefore, a more compact primitive would be better suited for this problem. In this context, conics, particularly circles, provide the most important clues to 3-D interpretation of images next to straight lines for the following reasons [1].

1) The conic is a more compact primitive than points and line segments, and it contains the pose information of a rigid-body object.
2) The representation of a conic is a symmetric matrix, which is easy to manipulate mathematically.
3) Circles have shown to have the important property of high image-location accuracy.
4) For motion analysis, no point-wise correspondence between two circles are necessary.

In general, motion and structure parameters cannot be estimated from only two images of a single conic [1]. Two images of at least three conics are needed in order to solve the complex nonlinear problem.

Manuscript received February 10, 1997; revised November 2, 1997 and December 7, 1997.

The authors are with the Computer Integrated Manufacturing Laboratory Department of Mechanical and Industrial Engineering, University of Toronto, Toronto, Ont., Canada M5S 3G8.

Publisher Item Identifier S 1083-4427(98)04349-5.

The active-vision system developed in our laboratory, for the recognition of moving objects, uses (artificial) circular features as targets to be tracked. In [8], we have shown that for a circle, with a known radius, a closed-form solution exists for determining its 3-D static pose from a single image, with the exception of having two possible orientations. A second image of the static circle is necessary to determine the true orientation based on the circle's eccentricity change. This suggests that, in general, for a circular feature of known size, two images may be sufficient to uniquely determine its 3-D general-motion parameters. No previous work, addressing this issue, has been reported in the literature.

In this paper, Section II will first briefly review the closed-form solution method presented in [8] for the (static) circular-feature pose-estimation problem. Subsequently, Section III will introduce the orientation-duality problem for features in motion and propose techniques to solve it using motion constraints or additional object features.

II. Pose Estimation of Circular Features

There have been several active-vision systems proposed in the literature for recognizing objects in motion [7], [9]–[14]. However, recognition techniques used by these systems are highly computationally intensive and sensitive to noise. Object preconditioning has been proposed in numerous occasions to help (static) object recognition systems in this regard [15], [16]. For the 3-D pose estimation of (static) circular features, for example, several approximate and exact solution methods have been proposed [8], [17], [18]. This paper is a follow-up to our own work on static-object recognition earlier reported in [8]. Thus, as previously mentioned, our current objective is "the use of circular features (i.e., markers) in the recognition of moving objects."

Circular features undergo perspective projection and would be perceived as elliptical shapes in arbitrarily acquired images. Estimation of the five elliptical parameters of this image is the first step toward the determination of the 3-D pose of the circular feature. These parameters can be obtained by using a least-squares type fitting technique [19].

The pose of a circular feature can be solved analytically [8]. First, based on the elliptical parameters of its image, the 3-D orientation is estimated; subsequently, based on the estimated orientation, the 3-D position of the feature is calculated.

Circular-feature pose estimation is equivalent to the solution of the following problem. Given a 3-D conic surface, defined by a base (the perspective projection of a circular feature in the image plane) and a vertex (the center of the camera's lens) with respect to a reference frame, determine the pose of the plane (with respect to the same reference frame), which intersects the cone and generates a circular curve (Fig. 1) [8].

The general form of the equation of a cone with respect to the image frame is as follows:

$$ax^2 + by^2 + cz^2 + 2fyx + 2gzx + 2hxy + 2ux + 2vy + 2wz + d = 0. \quad (1)$$

An intersection plane can be defined by $lx + my + nz = 0$. Therefore, the problem of finding the coefficients of the equation of a plane, for which the intersection is circular, can be expressed mathematically as: determine $l, m,$ and n such that the intersection of the conical surface with the following surface is a circle: $lx + my + nz = 0$, where $l^2 + m^2 + n^2 = 1$.

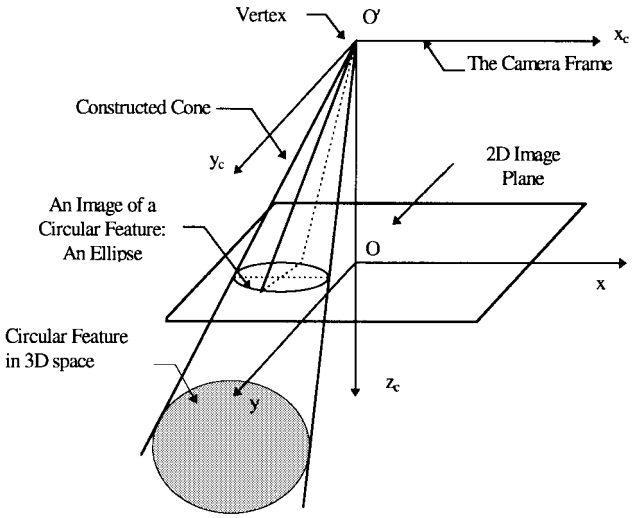

Fig. 1. Circular-feature pose estimation [8].

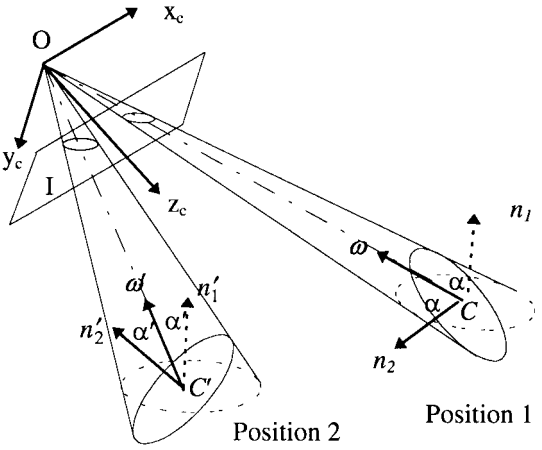

Fig. 2. Circular feature in translational motion.

The above 3-D orientation problem can be solved analytically by considering the equation of a cone in its central form, [24]. Thus, it is required to find the coefficients of the equation of a particular plane (with respect to the canonical XYZ-frame),

$$lX + mY + nZ = p \tag{2}$$

whose intersection with a central cone

$$\lambda_1 X^2 + \lambda_2 Y^2 + \lambda_3 Z^2 = 0 \tag{3}$$

would be a circle.

Three possible cases exist.

Case I: If $\lambda_1 < \lambda_2$, there exist four solutions to the problem. However, these are four symmetrical solutions with respect to the origin of the XYZ-frame and, consequently, represent only two unique solutions. If one takes the solutions on the positive section of Z-axis, then, the two solutions would be

$$\begin{aligned} n &= +\sqrt{\frac{\lambda_1 - \lambda_3}{\lambda_2 - \lambda_3}} \\ m &= \pm\sqrt{\frac{\lambda_2 - \lambda_1}{\lambda_2 - \lambda_3}} \\ l &= 0. \end{aligned} \tag{4}$$

Case II: If $\lambda_1 > \lambda_2$, following the same arguments for Case I, two solutions can be derived, which would be acceptable only if $\lambda_1 > \lambda_2$

$$\begin{aligned} n &= +\sqrt{\frac{\lambda_2 - \lambda_3}{\lambda_1 - \lambda_3}} \\ m &= 0 \\ l &= \pm\sqrt{\frac{\lambda_1 - \lambda_2}{\lambda_1 - \lambda_3}}. \end{aligned} \tag{5}$$

Case III: If $\lambda_1 = \lambda_2$, the equation of the central cone represents a right circular cone, (which implies that the central surface normal of the circular feature passes through the origin of the camera frame), and thus, intersection between any plane in the form $Z = k$ and the cone will generate a circular curve. Thus, there exists only one solution

$$\begin{aligned} n &= 1 \\ m &= 0 \\ l &= 0. \end{aligned} \tag{6}$$

It can be concluded that there exist two possible orientations. To obtain a unique acceptable solution, an extra geometrical constraint, such as the change of eccentricity in a second image, has to be obtained.

To solve for a unique solution for a marker's position, the radius of the circular feature has to be known. There exist two solutions: one on the positive Z-axis, and one the negative Z-axis [8]. Only the positive one is acceptable in our case (being located in front of the camera).

III. Solutions to the Orientation Duality Problem for Circular Features in Motion

The eccentricity of a circular feature's image acquired by a camera, whose focal axis is perfectly aligned with the circle's normal should be equal to one. Therefore, the change of eccentricity of the ellipse in the second image, acquired after a known movement of the camera, would yield the true orientation of the circular feature. This simple technique, however, can only be applied to static features.

For circular features in motion, several new effective techniques will be presented below to distinguish the true orientation from the false one via the use of consecutive images. In general, if a circular feature undergoes arbitrary 3-D motion, it is impossible to find its true orientation directly, since both orientations found at a specific position could be true under certain spatial transformation. In other words, without additional information, the true orientation of the feature cannot be determined from consecutive images. Two types of information are used herein to address this problem. One approach is to constrain the object motion, e.g., to consider only (pure) 3-D translation or planar motion. Another approach is to consider extra coplanar object features, other than the viewed circular-feature, such as points and lines, to provide structural information about the object.

A. 3-D Translation

An object is under (pure) translation in 3-D when no rotational motion exists about any axis. Fig. 2 depicts a circle moving from Position 1 to Position 2. At Position 1, we obtain two possible unit surface-normal vectors of the circle, $\boldsymbol{n_1}$ and $\boldsymbol{n_2}$. Likewise, we obtain $\boldsymbol{n_1'}$ and $\boldsymbol{n_2'}$ for the second image acquired at Position 2.

Conjecture 1: The true surface normal is the one that remains constant in both images.

Namely, if $\boldsymbol{n_1}$ is assumed to represent the true orientation, it would remain constant during the translation. (Here and in the following sections, the use of empirically defined thresholds is proposed for determining tangible changes in orientation vectors between consecutive images.)

Let ω and ω' define the unit directional vectors pointing from the circular-feature's center to the camera's focal point, which pass through the centers of the imaged ellipses. Based on Conjecture 1

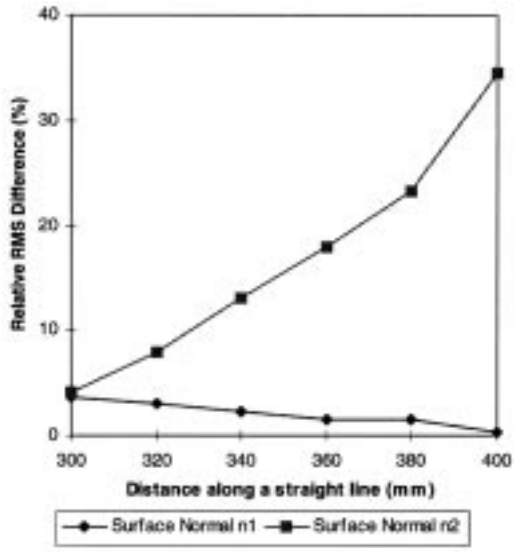

(a)

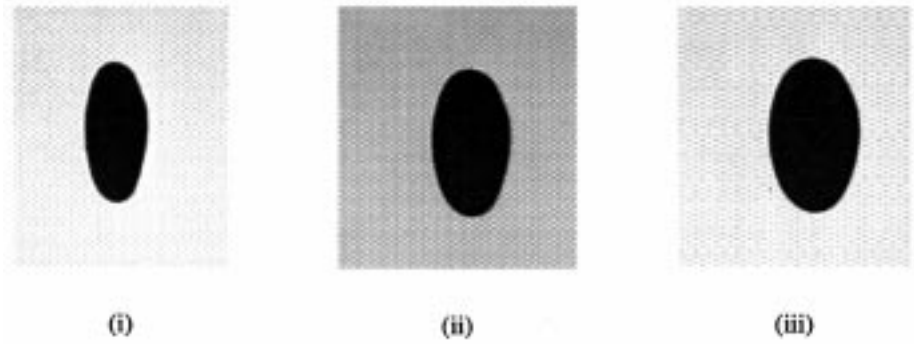

(b)

Fig. 3. Translation along the straight line: (a) experimental results and (b) three consecutive images.

and on the symmetry of the two possible orientations with respect to ω, a change in ω would necessarily imply a change in $\boldsymbol{n_2}$.

Ill-Conditioned Case: The false orientation of a circular feature changes, except when the circular marker is translating along a straight line toward the camera's focal center, i.e., when $\omega = \omega'$.

Let the axial unit vector ω be defined herein as follows:

$$\begin{aligned}\omega &= \frac{1}{\sqrt{(k_1+k_2)^2+(l_1+l_2)^2+(m_1+m_2)^2}} \\ &\quad \cdot [(k_1+k_2)\cdot i + (l_1+l_2)\cdot j + (m_1+m_2)\cdot k] \\ &= -\frac{1}{\sqrt{x_c^2+y_c^2+z_c^2}}(x_c\cdot i + y_c\cdot j + z_c\cdot k) \end{aligned} \tag{7}$$

where (x_c, y_c, z_c) represents Point C, (k_1, l_1, m_1) and (k_2, l_2, m_2) are the components of the orientation vectors $\boldsymbol{n_1}$ and $\boldsymbol{n_2}$, respectively, and $\boldsymbol{i}, \boldsymbol{j}$ and $\boldsymbol{k}$ are unit vectors, all defined with respect to the camera frame, Fig. 2.

Equation (7) can also be expressed in its component form as

$$\omega_x = k_1 + k_2 = -\sqrt{\frac{r^2}{x_c^2+y_c^2+z_c^2}}\cdot x_c \tag{8a}$$

$$\omega_y = l_1 + l_2 = -\sqrt{\frac{r^2}{x_c^2+y_c^2+z_c^2}}\cdot y_c \tag{8b}$$

$$\omega_z = m_1 + m_2 = -\sqrt{\frac{r^2}{x_c^2+y_c^2+z_c^2}}\cdot z_c \tag{8c}$$

where r is defined as

$$r^2 = (k_1+k_2)^2 + (l_1+l_2)^2 + (m_1+m_2)^2$$

and represents the magnitude of $\boldsymbol{\omega}$.

Similarly, for the second image, the vector $\boldsymbol{\omega}'$ is defined as

$$\omega_x' = k_1' + k_2' = -\sqrt{\frac{r'^2}{x_c'^2+y_c'^2+z_c'^2}}\cdot x_c' \tag{9a}$$

$$\omega_y' = l_1' + l_2' = -\sqrt{\frac{r'^2}{x_c'^2+y_c'^2+z_c'^2}}\cdot y_c' \tag{9b}$$

$$\omega_z' = m_1' + m_2' = -\sqrt{\frac{r'^2}{x_c'^2+y_c'^2+z_c'^2}}\cdot z_c'. \tag{9c}$$

When $\boldsymbol{n_1} = \boldsymbol{n_1'}$ and $\boldsymbol{n_2} = \boldsymbol{n_2'}$, in two consecutive images, the duality problem cannot be solved by the proposed technique. Then, by definition of ω and ω', we have

$$\omega = \omega'. \tag{10}$$

Equation (10) indicates that the problem is ill-conditioned when the object (purely) translates along the line OC.

Experiments:

Experimental Setup: The imaging system, used for all the experiments described in this paper, comprised a JVC CCD color camera (model TK-870U), with 510H × 492V pixels, mounted on a six degree-of-freedom GMF S100 robot's end effector; and,

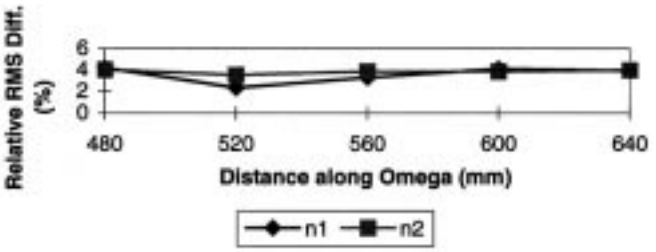

Fig. 4. Translation along ω.

a PC-based PIP-640B Matrox digitizer board with a 640 × 480 resolution. The camera was equipped with a 25 mm f/1.4 lens and normally placed 500 mm away from the circular features. The camera's extrinsic and intrinsic parameters were obtained using the mono-view, nonco-planar point technique proposed in [21]. Additional direct measurements were made to relate the camera's frame to the robot's base frame. Measurement errors in both x and y directions were less than 0.5%.

One must note that the selection of the camera's nominal distance to a circular feature is dependent on the feature's size. Also, the orientation of the camera must be chosen to maximize visibility of the feature. Both these issues were addressed in our earlier studies [22], [23] and the results implemented in this current work.

Experimental Procedure: Experiments were conducted to verify Conjecture 1 stated above. For increased accuracy, the mobile camera was translated along a certain 3-D path to simulate (feature's) translational motion, while the object itself was kept stationary. At several positions along the path, the possible surface normals of the circular marker on the object, $\boldsymbol{n_1}$ and $\boldsymbol{n_2}$, were estimated. The relative root-mean-square (rms) differences between the vectors and their initial values, i.e., $\|n_1 - n_1'\|/\|n_1\|$ and $\|n_2 - n_2'\|/\|n_2\|$, were calculated and recorded.

In the first test, the object pseudo-translated along a straight line that does not coincide with $\boldsymbol{\omega}$. The intervals between consecutive test positions were set at approximately 20 mm. At every instant, the RMS difference was calculated with respect to the original normals. As shown in Fig. 3, the relative rms differences in $\boldsymbol{n_2}$ are significantly greater than those in $\boldsymbol{n_1}$. The RMS-reduction trend of $\boldsymbol{n_1}$ in Fig. 3 is coincidental and primarily due to favorable alignment of the camera's optical axis with respect to the normal of the circular feature.

The expected ill-conditioned case was simulated by translating the camera away from the object along the vector $\boldsymbol{\omega}$. Measurements were taken at 40 mm intervals. The rms differences for this case, for both $\boldsymbol{n_1}$ and $\boldsymbol{n_2}$ are shown in Fig. 4. The results clearly show that both $\boldsymbol{n_1}$ and $\boldsymbol{n_2}$ remain relatively constant, and therefore the duality problem remains unsolved.

B. General Planar Motion

When a circular feature moves in a general planar motion, it has three degrees of freedom, (x, y, θ). Fig. 5 depicts a surface normal $\boldsymbol{n}$, which is translated from its initial position (x_c, y_c, z_c) to a new position (x_c', y_c', z_c'). It is rotated concurrently about the z axis by $\Delta\theta$. Namely, the vector $\boldsymbol{n}$ is transformed into $\boldsymbol{n}'$.

Since the motion is planar, the z component of the vector $\boldsymbol{n}$ will remain constant.

Conjecture 2: The z component of the false orientation vector changes, while that of the true orientation remains the same, with the exception of certain ill-conditioned cases.

Fig. 6 depicts Conjecture 2, stated above, where only a rotation about the z axis is considered. When the true surface normal $\boldsymbol{n_1}$ rotates around the z axis, the false solution $\boldsymbol{n_2}$ rotates correspondingly, so as to maintain the symmetry with respect to $\boldsymbol{\omega}$. Both vectors $\boldsymbol{n_1}$ and

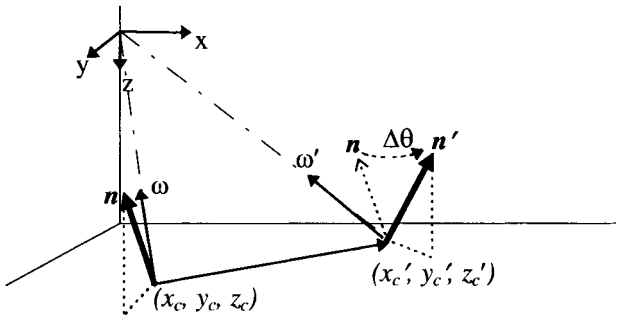

Fig. 5. Planar motion of the normal of a circular feature.

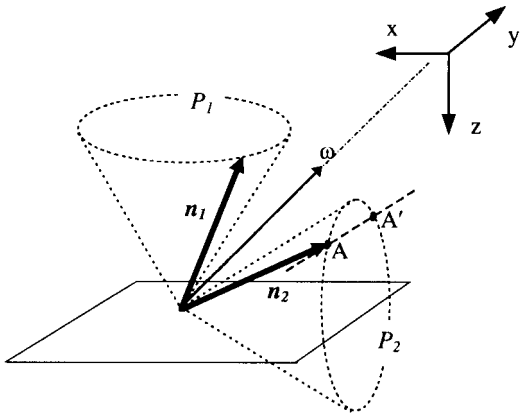

Fig. 6. Changes in the z component of $\boldsymbol{n_2}$.

$\boldsymbol{n_2}$ generate respective circular paths, P_1 and P_2. P_1 lies in a plane parallel to the feature-motion plane because only rotation about the z axis is permitted. Since $\boldsymbol{\omega}$ is an arbitrary vector, P_2 would normally lie in a plane that is not parallel to the feature-motion plane. Thus, a rotation of $\boldsymbol{n_1}$ and corresponding rotation of $\boldsymbol{n_2}$ would result in the change of the z component of $\boldsymbol{n_2}$.

The problem becomes ill-conditioned, when $\boldsymbol{n_2}$ maintains the same z component for a specific motion of $\boldsymbol{n_1}$. For every motion, there only exist two such possible positions on P_2, A and A$'$.

In light of this reasoning, the procedure for solving the orientation-duality problem for a circular feature moving in planar motion can be summarized as follows.

1) **Step 1:** Acquire the first image of the circular feature, and calculate: i) its center (x_c, y_c, z_c) and ii) the two possible orientation vectors $\boldsymbol{n_1}$ and $\boldsymbol{n_2}$.
2) **Step 2:** Check if the z components of both $\boldsymbol{n_1}$ and $\boldsymbol{n_2}$ are equal. If they are, i.e., $m_1 = m_2$, the proposed technique cannot be used, since $\boldsymbol{n_1}$ and $\boldsymbol{n_2}$ cannot be distinguished by their z components. We return to Step 1 to acquire a new image different than the first.

   Otherwise, i.e., $m_1 \neq m_2$, we proceed to Step 3.
3) **Step 3:** Acquire a second image of the same feature in motion (after a period of time), and, as in Step 1, calculate i) its center (x_c, y_c, z_c) and ii) the two possible orientation vectors $\boldsymbol{n_1'}$ and $\boldsymbol{n_2'}$.
4) **Step 4:** Compare the z components of the orientation vectors. If one of the z components remains constant between the two images, i.e., $m_1 = m_1'$, while the other one changes, i.e., $m_2 \neq m_2'$, the one that remains unchanged is the true solution. The duality problem is solved.

   Otherwise, i.e., both $m_1 = m_1'$, and $m_2 = m_2'$, the problem becomes *ill-conditioned*, and an additional image has to be acquired. The procedure returns to Step 3.

Ill-Conditioned Case: It is important to analytically determine the ill-conditioned case, under which the z components of both $\boldsymbol{n_1}$ and $\boldsymbol{n_2}$ remain constant, namely $m_1 = m_1'$ and $m_2 = m_2'$. Rearranging (8) (i.e., dividing (8a) and (8b) by (8c), and moving k_1 and l_1 to the right), k_2 and l_2 are expressed in terms of k_1 and l_1

$$k_2 = \frac{x_c}{z_c}(m_1 + m_2) - k_1$$
$$l_2 = \frac{y_c}{z_c}(m_1 + m_2) - l_1. \tag{11}$$

Since $\boldsymbol{n_1}$ and $\boldsymbol{n_2}$ represent unit vectors,

$$k_1^2 + l_1^2 + m_1^2 = 1$$
$$k_2^2 + l_2^2 + m_2^2 = 1. \tag{12}$$

The substitution of (11) into (12) yields

$$\left[\frac{x_c}{z_c}(m_1 + m_2) - k_1\right]^2 + \left[\frac{y_c}{z_c}(m_1 + m_2) - l_1\right]^2 + m_2^2 = 1. \tag{13}$$

Similarly, for Position 2 (in a general planar motion)

$$\left[\frac{x_c'}{z_c'}(m_1' + m_2') - k_1'\right]^2 + \left[\frac{y_c'}{z_c'}(m_1' + m_2') - l_1'\right]^2 + m_2'^2 = 1. \tag{14}$$

Since we assumed that $\boldsymbol{n_1}$ is the true solution,

$$\begin{bmatrix} k_1' \\ l_1' \end{bmatrix} = \begin{bmatrix} \cos\theta & -\sin\theta \\ \sin\theta & \cos\theta \end{bmatrix} \begin{bmatrix} k_1 \\ l_1 \end{bmatrix}, \qquad -\pi < \theta \le \pi. \tag{15}$$

Substituting $m_1 = m_1'$ and $m_2 = m_2'$ and (15) into (14), the following expression is obtained:

$$\left[\frac{x_c'}{z_c'}(m_1 + m_2) - (k_1\cos\theta - l_1\sin\theta)\right]^2 + \left[\frac{y_c'}{z_c'}(m_1 + m_2) - (k_1\sin\theta + l_1\cos\theta)\right]^2 + m_2^2 = 1. \tag{16}$$

Rearranging (16) into a standard form for circular curves, we obtain

$$\left[x_c' - \frac{z_c'}{(m_1 + m_2)}(k_1\cos\theta - l_1\sin\theta)\right]^2 + \left[y_c' - \frac{z_c'}{(m_1 + m_2)}(k_1\sin\theta + l_1\cos\theta)\right]^2 = \frac{z_c^2}{(m_1 + m_2)^2}\cdot(1 - m_2^2). \tag{17}$$

Equation (17) represents a group of circles, whose radius is

$$r_a = \frac{z_c'}{m_1 + m_2}\sqrt{(1 - m_2^2)} \tag{18}$$

and whose centers are located on another circle defined by

$$x = \frac{z_c}{m_1 + m_2}(k_1\cos\theta - l_1\sin\theta)$$
$$y = \frac{z_c}{m_1 + m_2}(k_1\sin\theta + l_1\cos\theta), \qquad -\pi < \theta \le \pi. \tag{19}$$

Thus, if (16) is satisfied by the motion at hand, an ill-conditioned problem results. The physical meaning of (16) is that, if the center of a circular feature moves from an arbitrary Position 1: (x_c, y_c, z_c) to a new Position 2: (x_c', y_c', z_c'), there exist two singular θ values for the rotation of the surface normal. These correspond to the two solutions of the quadratic (16).

It is worth noting that the singular θ angles are independent of the original position of the circular feature, whereas they depend on the original surface orientation $\boldsymbol{n_1}$ and the position of the second point B: (x_c', y_c', z_c').

Experiments: The experimental setup described earlier in Section III-A was used here as well to verify the validity of Conjecture 2. The object's translation was simulated by moving the camera parallel to the object's plane, whereas a rotation on this plane was achieved by turning the object manually to a desired angle utilizing an accurate setup. The parameters m_1 and m_2 were estimated at two different positions. The normalized relative (scalar) differences, based on the z values of $\boldsymbol{n_1}$ and $\boldsymbol{n_2}$, $(m_1 - m_1'/m_1)$ and $m_2 - m_2'/m_2$, were then calculated.

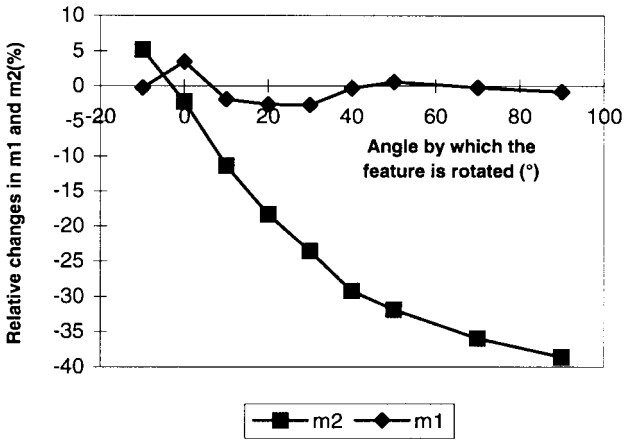

Fig. 7. Changes in m_1 and m_2 in planar motion.

Fig. 7 provides an example of a circular feature in planar motion. The position of the feature's center is pseudo-translated from Position 1: [0, −50, 0] (mm) to Position 2: [0, 0, 0] (mm). Relative changes in m_1 and m_2 were measured with respect to Position 1. We observe that the change in m_2 is significant, except in the $-10^\circ \sim 0^\circ$ range. Applying (16), the singular value θ^* is calculated to be -5.0°. This θ^* value is in agreement with the experimental value noted in Fig. 7.

C. General Motion—Consideration of Additional Features

The orientation duality problem cannot be solved for a 3-D general motion without considering additional information. The reasoning behind the approach of using additional features is similar to those of the solution proposed in Sections III-A and III-B for constrained motions, namely, to find a parameter which remains constant, for the true orientation, over consecutive images, while changing for the false one.

In the case of a constrained motion, we used the feature's normal vector itself, or simply its z component, as the invariant to distinguish the true solution from the false one. Similarly, here, for a "rigid-body" object in 3-D general motion, we use the fact that the relative distances among all the points on the object remain constant. However, we do not assume that these distances are known *a priori*.

1) A Coplanar Point: Consideration of an object point coplanar with the circular feature can lead to the solution of the orientation-duality problem. This coplanar point can, for example, be a corner point on the same object plane as the circular-feature and visible in the same image plane. Based on the rigid-body constraint, the distance between the point-feature and circular-feature's center, although unknown at the time of image acquisition and analysis, must remain constant in consecutive images. The concept is illustrated in Fig. 8.

Depicted in Fig. 8 is a circular feature moving from Position 1 to Position 2 in an arbitrary motion. Let P_t and P_t' be the same "true" point-feature on the object at Positions 1 and Position 2, respectively, and, let P_i and P_i' be the corresponding points on the image plane I, defined by (x_i, y_i, f) and (x_i', y_i', f), where f is the focal-length of the camera. Also, let points P_f and P_f' be the estimated false position of the point-feature in both images, resulting from the orientation-duality problem. In Fig. 8, d_1 is the distance between the true point

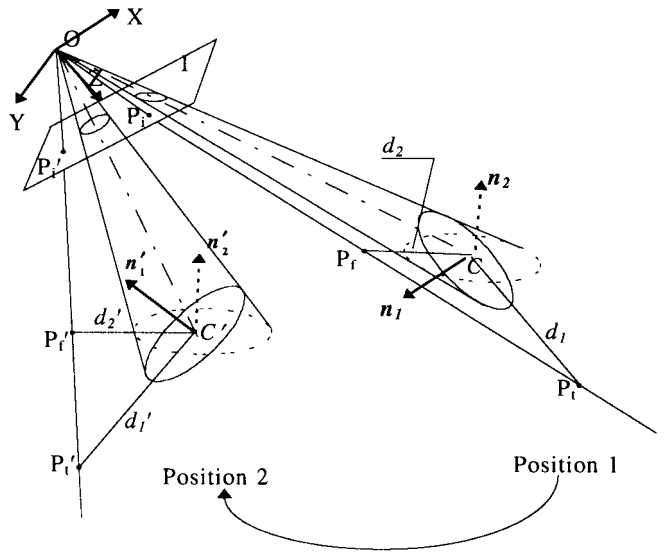

Fig. 8. Solution for the orientation duality problem: considering a coplanar point.

P_t and the circular-feature's center C, and d_2 is the distance to the false point P_f. We define d_1' and d_2' in the same fashion for the second image.

Conjecture 3: Since all the points on a rigid body remain at constant distances with respect to one another, the distance between the point feature and the circular-feature's center at Position 1 should be equal to that at Position 2, i.e.,

$$d_1 = d_1' \tag{20}$$

while

$$d_2 \neq d_2'. \tag{21}$$

It will be shown that, Conjecture 3, described by (20) and Inequality (21), is always satisfied with a limited number of exceptions. For the solution of the orientation duality problem using this conjecture, the distances d_1, d_2, d_1', and d_2' must be first calculated. Based on the constraint that the point under consideration is coplanar with the circular feature, the following equations can be established:

$$\boldsymbol{p_t} \cdot \boldsymbol{n}_1 = 0 \tag{22}$$

$$\boldsymbol{p_f} \cdot \boldsymbol{n}_2 = 0 \tag{23}$$

$$\boldsymbol{p_t'} \cdot \boldsymbol{n}_1' = 0 \tag{24}$$

$$\boldsymbol{p_f'} \cdot \boldsymbol{n}_2' = 0 \tag{25}$$

where $\boldsymbol{p_t}, \boldsymbol{p_f}, \boldsymbol{p_t'}$ and $\boldsymbol{p_f'}$ are defined as the "distance" vectors, with respect to the camera frame, pointing from C to points P_t, P_f, P_t', and P_f', respectively.

Similarly, another set of vectors, $\boldsymbol{r_t}, \boldsymbol{r_f}, \boldsymbol{r_t'}$, and $\boldsymbol{r_f'}$, can be defined as pointing from the camera's origin, Point O, to P_t, P_f, P_t', and P_f', respectively. Lying on the same lines of sight, OP_i and OP_i', these vectors can be related to the vectors, $\boldsymbol{r_i}$ and $\boldsymbol{r_i'}$, pointing from O to P_i and P_i', as follows:

$$\boldsymbol{r_t} = s_1 \boldsymbol{r_i} \tag{26a}$$

$$\boldsymbol{r_f} = s_2 \boldsymbol{r}_i \tag{26b}$$

$$\boldsymbol{r_t'} = s_1' \boldsymbol{r_i'} \tag{26c}$$

$$\boldsymbol{r_f'} = s_2' \boldsymbol{r_i'} \tag{26d}$$

where s_1, s_2, s_1', and s_2' are simply scaling factors. Since vectors $\boldsymbol{r_i}$ and $\boldsymbol{r_i'}$ are determined by locating the coordinates of P_i and P_i' in the image plane I, the positions for the point-feature, P_t and P_f, can be determined by solving for s_1, s_2, s_1', and s_2'.

Substituting (26) into (22)–(25), and expressing the vectors in terms of their components, we obtain

$$s_1 = \frac{k_1 x_c + l_1 y_c + m_1 z_c}{k_1 x_i + l_1 y_i + m_1 f}$$
$$s_2 = \frac{k_2 x_c + l_2 y_c + m_2 z_c}{k_2 x_i + l_2 y_i + m_2 f} \tag{27a}$$

and

$$s_1' = \frac{k_1' x_c' + l_1' y_c' + m_1' z_c'}{k_1' x_i' + l_1' y_i' + m_1' f}$$
$$s_2' = \frac{k_2' x_c' + l_2' y_c' + m_2' z_c'}{k_2' x_i' + l_2' y_i' + m_2' f}. \tag{27b}$$

Therefore, the different positions of the point feature, in the camera frame, are expressed as follows:

$$P_t = s_1(x_i, y_i, f)$$
$$P_f = s_2(x_i, y_i, f) \tag{28a}$$

and

$$P_t' = s_1'(x_i', y_i', f)$$
$$P_f' = s_2'(x_i', y_i', f). \tag{28b}$$

The distances between the point-feature and the circular-feature's center can now be calculated as

$$d_1^2 = (x_1 x_i - x_c)^2 + (s_1 y_i - y_c)^2 + (s_1 f - z_c)^2$$
$$d_2^2 = (x_2 x_i - x_c)^2 + (s_2 y_i - y_c)^2 + (s_2 f - z_c)^2, \tag{29a}$$

and

$$d_1'^2 = (s_1' x_i' - x_c')^2 + (s_1' y_i' - y_c')^2 + (s_1' f - z_c')^2$$
$$d_2'^2 = (s_2' x_i' - x_c')^2 + (s_2' y_i' - y_c')^2 + (s_2' f - z_c')^2. \tag{29b}$$

The procedure of solving the duality problem with one additional coplanar point-feature can be summarized as follows.

1) **Step 1:** Acquire the first image of the object and determine i) the circular-feature's center (x_c, y_c, z_c), ii) the two possible orientations $\boldsymbol{n_1}$ and $\boldsymbol{n_2}$, and iii) the image coordinates of the additional point feature (x_i, y_i, f).
2) **Step 2:** Solve for the two possible positions of the point-feature, P_t and P_f, using (28a).
3) **Step 3:** Apply (29a) to calculate the distances between the two possible point features and the circular-feature's center, namely d_1 and d_2.
4) **Step 4:** Acquire a second image of the object and repeat Steps 1–3 to determine P_t' and P_f' using (28b), and d_1' and d_2' using (29b).
5) **Step 5:** Check whether $d_1 = d_1'$ and $d_2 \neq d_2'$; if true, then $\boldsymbol{n_1}, \boldsymbol{n_1'}$ must be the true orientations of the circular feature, while P_t and P_t' are the true positions of the point feature. Thus, the duality problem is solved.

   If, however, both $d_1 = d_1'$ and $d_2 = d_2'$, the duality problem is ill-conditioned, and a third image is necessary.

Ill-Conditioned Case: In order to determine analytically when the ill-conditioned case occurs, the problem is formulated here as follows. Given a rigid-body object, with a circular feature and a point feature on one of its surfaces, moving from Position 1 to Position 2, what values of $\boldsymbol{n_1'}$ and $\boldsymbol{n_2'}$, will result in an ill-conditioned problem, i.e., for which $d_1 = d_1'$ and $d_2 = d_2'$?

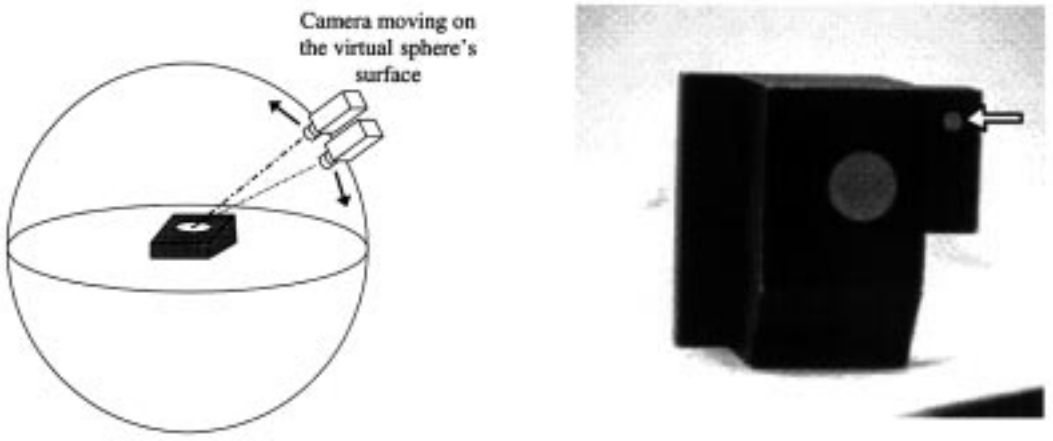

(a) (b)

Fig. 9. (a) Three-dimensional camera movement and (b) artificial features.

In mathematical terms, the above implies solving for s_1' and s_2' in the following, which are obtained by equating (29a) and (29b)

$$d_1'^2 = (s_1'x_i' - x_c')^2 + (x_1'y_i' - y_c')^2 + (s_1'f - z_c')^2 = d_1^2 \tag{30a}$$

and

$$d_2'^2 = (s_2'x_i' - x_c')^2 + (s_2'y_i' - y_c')^2 + (s_2'f - z_c')^2 = d_2^2. \tag{30b}$$

Since the only unknown in (30a) is s_1', and the only unknown in (30-b) is s_2', we can solve for s_1' and s_2' individually. As scaling factors, s_1' and s_2' must have real values. Since $\boldsymbol{n_1}$ and $\boldsymbol{n_1'}$ are assumed to be the true orientations for the circular feature, there must exist real roots for (30a). For (30b), however, real solutions for s_2' might not exist. Therefore, the ill-conditioned problem can only occur when there is a real solution for s_2' in (30b).

Once the values of s_1' and s_2' (assuming s_2' has a real solution) are obtained, we can solve for $\boldsymbol{n_1'}$ and $\boldsymbol{n_2'}$ that satisfy the ill-conditioned problem. Rearranging [(27a) and (27b)], by moving the denominator of the right-hand side to the left and moving all the terms to the left, we obtain

$$k_1'(x_c' - s_1'x_i') + l_1'(y_c' - s_1'y_i') + m_1'(z_c' - s_1'f) = 0 \tag{31a}$$

and

$$k_2'(x_c' - s_2'x_i') + l_2'(y_c' - s_2'y_i') + m_2'(z_c' - s_2'f) = 0. \tag{31b}$$

In the above equations, there are six unknowns, three for $\boldsymbol{n_1'}(k_1', l_1', m_1')$ and three for $\boldsymbol{n_2'}(k_2', l_2', m_2')$.

Based on the symmetry of the two orientations for the circular-feature, we can obtain four more equations

$$k' - 1 + k_2' = (m_1' + m_2')\frac{x_c'}{z_c'} \tag{31c}$$

$$l_1' + l_2' = (m_1' + m_2')\frac{y_c'}{z' - c} \tag{31d}$$

$$k_1'^2 + l_1'^2 + m_1'^2 = 1, \quad \text{and} \tag{31e}$$

$$k_2'^2 + l_2'^2 + m_2'^2 = 1. \tag{31f}$$

Combining (31a)–(31f), we have six equations and six unknowns. The first four equations are linear, while the last two are quadratic.

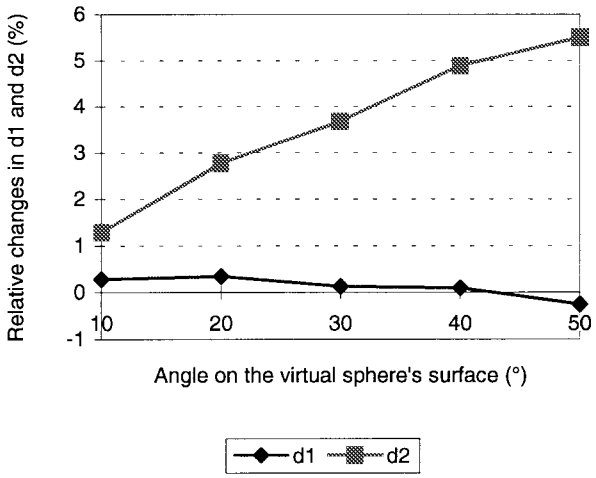

Fig. 10. Changes in the distance d_1 and d_2 when the camera is moved on the sphere's surface.

By Bezout's Theorem [14], since all (31) are independent, there exist $1^4 \cdot 2^2 = 4$ solutions. As (k_1', l_1', m_1') and (k_2', l_2', m_2') are feature orientations, only real solutions are acceptable. The number of acceptable orientations should therefore be less than four. In other words, when the object moves from Position 1 to Position 2 in a general motion, there would not be more than four possible orientations of the object that would result in an ill-conditioned problem for the detection of the true orientation of the circular-feature.

Experiments: Conjecture 3 was verified experimentally using an object with a circular feature and an artificial coplanar point feature. The object motion was simulated by moving the camera on a virtual sphere's surface, with the camera always pointing toward the circular feature's center to maximize visibility (Fig. 9) [22].

Following Steps 1–4 stated above, the relative changes in the parameters d_1 and d_2, i.e., $d_1' - d_1/d_1$ and $d_2' - d_2/d_2$, were calculated and plotted in Fig. 10, for 10°-incremented camera movements. As can be noted, changes in d_1 remain almost constant, while changes in d_2 vary significantly. Thus, d_1 is clearly the true solution.

In another example, the camera was moved along the radius of the sphere toward the object [24]. As in the case of motion over the sphere's surface, changes in d_2 were significant, while changes in d_1 remained relatively constant. It was noted that, the rate of change

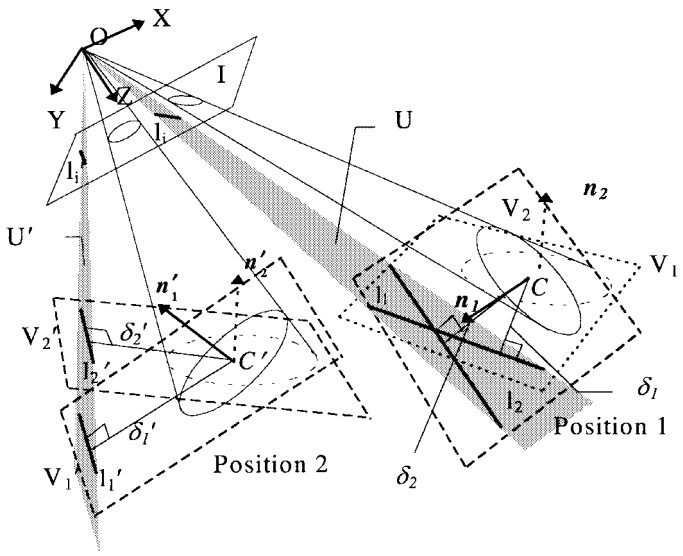

Fig. 11. Solution for the duality problem with an additional line-feature.

in d_2 was higher at closer camera distances to the object. Thus, one must operate in an optimal distance range in order to determine the true feature orientation with high confidence.

2) A Coplanar Line: Since the object in motion is assumed to be a rigid body, the distance between a coplanar line feature and the circular-feature's center can be used as an invariant to solve the duality problem, even though its value is not known a priori. In this section, we assume that a coplanar linear edge has already been extracted from the image using common edge detectors, and that its mathematical form has also been determined. Fig. 11 depicts an object motion from Position 1 to Position 2.l_1 and l_1' are the line-features on the object in Positions 1 and 2, respectively, while l_2 and l_2' are the corresponding possible lines due to the orientation duality. l_i and l_i' are the projections of the same lines in the image Plane I in the two consecutive images.

The parameter δ_1 is defined as the shortest distance between the line-feature l_1 and the circular-feature's center C. Similarly, δ_2, δ_1' and δ_2' represent corresponding distances between the line-feature and the circular-feature's center.

Conjecture 4: Since the object is assumed to be a rigid body, i.e., the distances among all the points on the object surface remain constant during object motion

$$\delta_1 = \delta' - 1 \tag{32}$$

if one assumes that l_1 is the true position of the line feature. On the other hand, it will be shown that, with a limited number of exceptions

$$\delta_2 \neq \delta_2'. \tag{33}$$

To use Conjecture 4, defined by (32) and Inequality (33), $\delta_1, \delta_2, \delta_1'$, and δ_2' have to be calculated first. Knowing the camera's focal length, f, the image plane I can be defined at $z = f$ with respect to the camera frame (Fig. 11). The projection of the line-feature l_i within the plane I can be defined by

$$ax + by + c = 0. \tag{34}$$

Let us define the plane that passes through both the focal point O and Line l_i as Plane U, and the planes on which the circular feature possibly lies as Planes V_1 and V_2. Since the line-feature must lie in Plane U, also given that the line and the circular-feature are coplanar, we can solve for the line positions by intersecting Plane U with Planes V_1 and V_2.

First, we obtain the equation for Plane U as

$$ax + by + \frac{c}{f}z = 0. \tag{35}$$

To simplify the last coefficient of the equation, let $f = 1$. Equation (35), with a modified constant, c, is then reduced to

$$ax + by + cz = 0. \tag{36}$$

Similarly, at Position 2, for Line l_i'

$$a'x + b'y + c' = 0 \tag{37}$$

and for Plane U'

$$a'x + b'y + c'z = 0. \tag{38}$$

The orientations of Planes V_1 and V_2 are defined by unit surface normals, $\boldsymbol{n_1}$ and $\boldsymbol{n_2}$. Plane V_1 can then be expressed by

$$k_1(x - x_c) + l_1(y - y_c) + m_1(z - z_c) = 0, \tag{39}$$

where (k_1, l_1, m_1) are the components of $\boldsymbol{n_1}$, and (x_c, y_c, z_c) are the coordinates of the circular-feature's center. After collecting all the constant terms, (39) is reduced to

$$k_1x + l_1y + m_1z + w_1 = 0 \tag{40}$$

where parameter w_1 is defined by

$$w_1 = -k_1x_c - l_1y_c - m_1z_c. \tag{41}$$

Similarly, for Plane V_2, we have

$$k_2x + l_2y + m_2z + w_2 = 0 \tag{42}$$

where parameter w_2 is defined by

$$w_2 = -k_1x_c - l_1y_c - m_1z_c. \tag{43}$$

The intersection of Plane U and Plane V_1 yields Line l_1 in the following form:

$$\frac{N_1x - bw_1}{L_1} = \frac{N_1y + w_1a}{M_1} = z \tag{44}$$

where

$$L_1 = \begin{vmatrix} b & c \\ l_1 & m_1 \end{vmatrix}$$
$$M_1 = \begin{vmatrix} c & a \\ m_1 & k_1 \end{vmatrix}$$
$$N_1 = \begin{vmatrix} a & b \\ k_1 & l_1 \end{vmatrix}.$$

Similarly, the equation for Line l_2 is obtained as

$$\frac{N_2x - bw_2}{L_2} = \frac{N_2y + w_2a}{M_2} = z \tag{45}$$

where

$$L_2 = \begin{vmatrix} b & c \\ l_2 & m_2 \end{vmatrix}$$
$$M_2 = \begin{vmatrix} c & a \\ m_2 & k_2 \end{vmatrix}$$
$$N_2 = \begin{vmatrix} a & b \\ k_2 & l_2 \end{vmatrix}.$$

For Position 2, l_1' and l_2' can be acquired in the same fashion. Once the line equations are determined, the distances $\delta_1, \delta_2, \delta_1'$, and δ_2' can be calculated [14]. For Position 1, and $\boldsymbol{n_1}$, we have

$$\delta_1^2 = \frac{1}{L_1^2 + M_1^2 + N_1^2}[(y_cN_1 - z_cM1 + aw_1)^2 + (z_cL_1 - x_cN_1 + bw_1)^2 + (x_cM_1 - y_cL_1 + cw_1)^2]. \tag{46}$$

δ_2, δ_1', and δ_2' can be calculated similarly. Using (32) and Inequality (33), we can determine the true surface orientation.

The procedure of solving the duality problem with one additional coplanar line-feature can be summarized as follows.

1) **Step 1:** Acquire the first image of the object, extract a line-feature and represent it in the form of (34). Calculate i) the circular-feature's center (x_c, y_c, z_c) and ii) the two possible orientations, $\boldsymbol{n_1}$ and $\boldsymbol{n_2}$, for the same circular-feature. The parameters a, b, c, w_1, and w_2 are subsequently determined.
2) **Step 2:** Solve for the possible 3-D position of the line-features, using (44) and (45). The parameters L_1, M_1, N_1, L_2, M_2, and N_2 are then calculated.
3) **Step 3:** Apply (46) to calculate the distances between the line-feature and circular-feature's center, δ_1 and δ_2.
4) **Step 4:** Acquire a second image of the object. Follow the same steps as for the first image, to solve for l_1', l_2', δ_1', and δ_2', (Steps 1–3).
5) **Step 5:** Compare δ_1 and δ_2 with δ_1' and δ_2', if both (32) and Inequality (33) are satisfied, $\boldsymbol{n_1}$ and $\boldsymbol{n_1}$ would be the true orientations of the circular feature. Also, l_1 and l_1' would be the true positions of the line feature. Thus, the duality problem is solved.

   If, however, Inequality (33) is not satisfied, i.e.,

$$\delta_1' = \delta_2' \tag{47}$$

   the duality problem cannot be solved. This situation is an *ill-conditioned problem*. Similar to the previous cases, a third image is needed to solve the ill-conditioned duality problem.

Ill-Conditioned Case: When the object is first moved to Position 1, the values of δ_1 and δ_2 are determined. For the problem to become ill-conditioned, δ_1' and δ_2', at Position 2, have to be equal to δ_1 and δ_2, respectively. Therefore, the following equations, obtained by combining (32), (33), (46), and (47), must be satisfied:

$$\begin{aligned}\delta_1^2 &= \delta_1'^2 \\ &= \frac{1}{L_1'^2 + M_1'^2 + N_1'^2}[(y_c'N_1' - z' - cM_1' + a'w_1')^2 \\ &\quad + (z_c'L_1' - x_c'N_1' + b'w_1')^2 \\ &\quad + (x_c'M_1' - y_c'L_1' + c'w_1')^2] \end{aligned} \tag{48a}$$

and

$$\begin{aligned}\delta_2^2 &= \delta_2'^2 \\ &= \frac{1}{L_2'^2 + M_2'^2 + N_2'^2}[(y_c'N_2' - z_c'M_2' + a'w_2')^2 \\ &\quad + (z_c'L_2' - x_c'N_2' + b'w_2')^2 \\ &\quad + (x_c'M_2' - y_c'L_2' + c'w_2')^2]. \end{aligned} \tag{48b}$$

Based on the relationships in (44) and (45), there exist three unknowns $(k_1', l_1'$, and $m_1')$ in (48a), and three unknowns $(k_2', l_2'$, and $m_2')$ in (48b). Due to the symmetry condition of $\boldsymbol{n_1'}$ and $\boldsymbol{n_2'}$:

$$k_1' + k_2' = (m_1' + m_2')\frac{x_c'}{z_c'}, \tag{48c}$$

$$l_1' + l_2' = (m_1' + m_2')\frac{y_c'}{z_c'} \tag{48d}$$

and, since $\boldsymbol{n_1'}$ and $\boldsymbol{n_2'}$ are unit vectors,

$$k_1'^2 + l_1'^2 + m_1'^2 = 1 \tag{48e}$$

$$k_2'^2 + l_2'^2 + m_2'^2 = 1. \tag{48f}$$

The set of (48) comprises six equations for six unknowns. The roots of this set of equations, (k_1', l_1', m_1') and (k_2', l_2', m_2'), are the singular orientations of the circular feature that result in the ill-conditioned problem. Based on Bezout's Theorem [14], since each equality in (48) is independent of one another, there exist $2^4 \cdot 1^2 = 16$ solutions. (k_1', l_1', m_1') and (k_2', l_2', m_2') being orientations of the circular feature, only real solutions are allowed. Therefore, there should be no more than 16 possible orientations that will result in an ill-conditioned problem for the detection of the true orientation of the features.

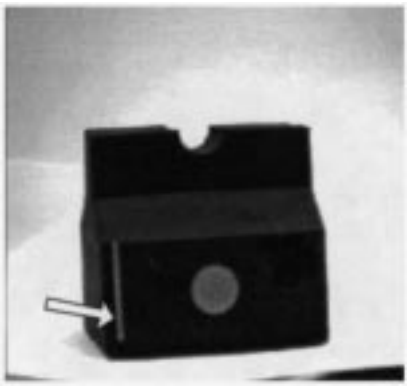

Fig. 12. Artificial features.

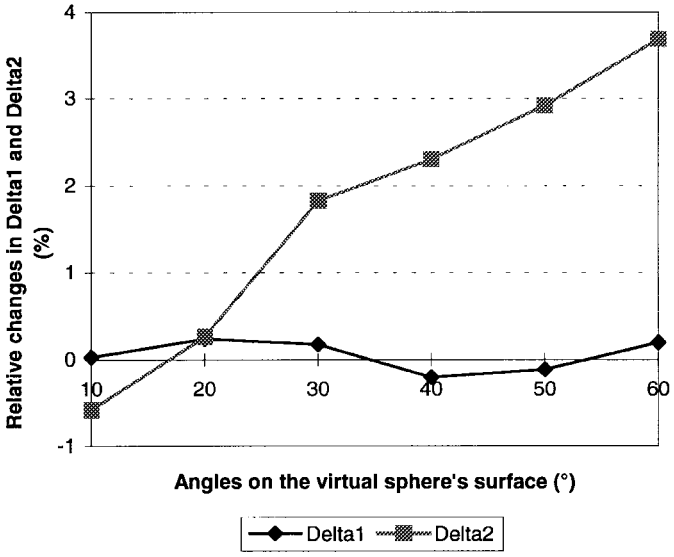

Fig. 13. Changes in δ_1 and δ_2, when the camera is moving on a virtual sphere's surface.

Experiments: Conjecture 4 was verified experimentally using an object with coplanar (artificial) circular and linear features (Fig. 12). The camera was moved in the same fashion as depicted in Fig. 9. Fig. 13 is a plot of relative changes in δ_1 and δ_2 at different test positions, when the camera was moved on the sphere's surface at 10° increments. As can be noted, δ_1 remains relatively constant, while δ_2 changes significantly as the object moves away from the initial position.

IV. Discussion and Conclusions

Circular features have been commonly used in computer-vision-based object recognition. In this paper, we advocate their usefulness in object-motion estimation. However, although a circular feature's position can be obtained from a single image, at least two consecutive images would be necessary to solve the orientation-duality problem. For objects in motion, this requirement poses a challenging task. The first solution presented in this paper is applicable to constrained

motions, which would be typical for industrial settings: i) motion along 3-D straight lines, and ii) general planar motion. The proposed conjectures were shown to be reliable via experimentation with real object surfaces that were marked with artificial circular markers.

The second solution approach, for 3-D general motion, advocates the use of additional features, which are coplanar to the circular features monitored. Based on the assumption that the marked object is a rigid body, the distances from a circular feature to such additional features, though unknown a priori, can be used as invariants to solve the duality problem. Experiments also showed that these methods are effective in practice.

Ill-conditioned positions do exist for all solutions proposed in this paper. However, they can be found by solving a set of linear and quadratic equations, and normally eliminated during run-time by acquiring a third image of the moving object.

The solution methods outlined herein were successfully utilized within our active-vision based moving-object recognition scheme [25].

REFERENCES

[1] S. D. Ma, "Conics-based stereo, motion estimation, and pose determination," *Int. J. Comput. Vision*, vol. 10, no. 1, pp. 7–25, 1993.

[2] M. Yamamoto and K. Ikeda, "Stereoscopic correcting pose of 3-D model of object," *Time-Varying Image Processing and Moving Object Recognition*, V. Cappelini, Ed. Amsterdam, The Netherlands: Elsevier, 1994, vol. 3, pp. 127–134.

[3] T. S. Huang and A. N. Netravali, "Motion and structure from feature correspondence: A review," *Proc. IEEE*, vol. 82, pp. 252–268, Feb. 1994.

[4] Y. C. Liu and T. S. Huang, "Estimation of rigid body motion using straight line correspondences," in *IEEE Workshop Motion*, Kiawah Island, SC, 1986, pp. 47–52.

[5] M. E. Spetsakis and J. Aloimonos, "Close form solutions to the structure from motion problem from line correspondence," in *Proc. AAAI*, Seattle, WA, 1987, pp. 738–743.

[6] J. K. Aggarwal and Y. F. Wang, "Analysis of a sequence of images using point and line correspondence," in *Int. Conf. Robotics Automation*, Raleigh, NC, 1987, pp. 1275–1280.

[7] J. K. Aggarwal and N. Nandhakumar, "On the computation of motion from sequence of images: A review," *Proc. IEEE*, vol. 76, pp. 971–935, Aug. 1988.

[8] R. Safaee-Rad, K. C. Smith, B. Benhabib, and I. Tchoukanov, "3-D location estimation of circular features for machine vision," *IEEE Trans. Robot. Automat.*, vol. 8, pp. 624–640, Oct. 1992.

[9] G. L. Foresti and V. Murino, "Moving-object recognition from an image sequence for autonomous vehicle driving," in *Time-Varying Image Processing and Moving Object Recognition*, V. Cappelini, Ed. Amsterdam, The Netherlands: Elsevier, 1994, vol. 3, pp. 383–390.

[10] M. Yamamoto, "Pose from motion: A direct method," in *Time-Varying Image Processing and Moving Object Recognition*, V. Cappelini, Ed. Amsterdam, The Netherlands: Elsevier, 1994, vol. 3, pp. 287–294.

[11] J. Hwang, Y. Ooi, and S. Ozawa, "An adaptive sensing system with tracking and zooming a moving object," *IEICE Trans. Inform. Syst.*, vol. E76-D, pp. 926–934, Aug. 1993.

[12] D. Murray and A. Basu, "Active tracking," in *IEEE Int. Conf. Intelligent Robots Systems*, Yokohama, Japan, 1993, pp. 1021–1028.

[13] S. Shmuel and M. Werman, "Active vision: 3-D from an image sequence," in *IEEE Int. Conf. Pattern Recognition*, Atlantic City, NJ, 1990, vol. 1, pp. 8–54.

[14] J. T. Feddema and C. S. G. Lee, "Adaptive image feature prediction and control for visual tracking with a hand-eye coordinated camera," *IEEE Trans. Syst., Man, Cybern.*, vol. 20, pp. 1172–1183, Sept./Oct. 1990.

[15] M. J. Magee and J. K. Aggarwal, "Determine the position of a robot using a single calibration object," *IEEE Int. Conf. Robotics Automation*, Atlanta, GA, 1984, pp. 140–149.

[16] B. Ussain and M. R. Kabuka, "Real-time system for accurate three-dimensional position determination and verification," *IEEE Trans. Robot. Automat.*, vol. 6, pp. 31–43, Feb. 1990.

[17] Y. Fainman, L. Feng, and Y. Koren, "Estimation of absolute spatial position of mobile systems by hybrid opto-electronic processor," *IEEE, Int. Conf. Systems, Man, Cybernetics*, Cambridge, MA, 1989, pp. 651–657.

[18] Y. C. Shin and S. Ahmad, "3D location of circular spherical features by monocular model-based vision," *IEEE Int. Conf. Syst., Man, Cybern.*, Boston, MA, 1989, pp. 576–581.

[19] R. Safaee-Rad, K. C. Smith, B. Benhabib, and I. Tchoukanov, "Accurate estimate of quadratic curves from grey-level images," *J. Comput. Vision, Graphics, Image Processing: Image Understanding*, vol. 54, pp. 259–274, Sept. 1991.

[20] N. Ayache and O. D. Faugeras, "HYPER: A new approach for the recognition and positioning of two-dimensional objects," *IEEE Trans. Pattern Anal. Machine Intell.*, vol. PAMI-8, no. 1, pp. 44–54, 1986.

[21] R. Y. Tsai, "A versatile camera calibration technique for high-accuracy 3-D machine vision metrology using off-the-shelf TV cameras and lenses," *IEEE J. Robot. Automat.*, vol. RA-3, pp. 323–344, Aug. 1987.

[22] X. He, B. Benhabib, and K. C. Smith, "CAD-based off-line planning for active vision," *J. Robot. Syst.*, vol. 12, pp. 677–691, Oct. 1995.

[23] R. Safaee-Rad, "An active vision system for 3-D object recognition in robotic assembly workcells," Ph.D. dissertation, Dept. Mech. Eng., Univ. Toronto, Toronto, Ont., Canada, 1991.

[24] D. He, "An active-vision system for the recognition of moving objects, M.A.Sc. thesis, Dept. Mech. Eng., Univ. Toronto, Toronto, Ont., Canada, 1996.

[25] D. He, D. Hujic, J. K. Mills, and B. Benhabib, "Moving object recognition using pre-marking and active vision system," in *IEEE Int. Conf. Robotics Automation*, Minneapolis, MN, 1996, pp. 1980–1985.

Sufficient Conditions on Uniform Approximation of Multivariate Functions by General Takagi–Sugeno Fuzzy Systems with Linear Rule Consequent

Hao Ying

***Abstract*—We have constructively proved a general class of multi-input single-output Takagi–Sugeno fuzzy systems to be universal approximators. The systems use any types of continuous fuzzy sets, any types of fuzzy logic AND, fuzzy rules with linear rule consequent and the generalized defuzzifier. We first prove that the TS fuzzy systems can uniformly approximate any multivariate polynomial arbitrarily well, and then prove they can uniformly approximate any multivariate continuous function arbitrarily well. We have derived a formula for computing the minimal upper bounds on the number of fuzzy sets and fuzzy rules necessary to achieve prespecified approximation accuracy for any given bivariate function. A numerical example is furnished. Our results provide a solid theoretical basis for fuzzy system applications, particularly as fuzzy controllers and models.**

I. INTRODUCTION

With respect to fuzzy control and modeling applications, the existing fuzzy systems can be classified into two major types, namely Mamdani fuzzy systems and Takagi–Sugeno (TS) fuzzy systems. The primary difference between them lies in the fuzzy rule consequent. Mamdani fuzzy systems use fuzzy sets as rule consequent whereas

Manuscript received April 20, 1997; revised December 7, 1997. This work was supported in part by a Biomedical Engineering Research Grant from The Whitaker Foundation and by the Texas Higher Education Coordinating Board under Grant 004952-054.

The author is with the Department of Physiology and Biophysics, Biomedical Engineering Center, The University of Texas Medical Branch, Galveston, TX 77555-0456 USA (e-mail: hying@utmb.edu).

Publisher Item Identifier S 1083-4427(98)04348-3.